2015 IEEE International Conference on Systems, Man, and Cybernetics

Mutual Information based Risk-aware Active Sensing in An Urban Environment

Z. Kan, C. Ton, M. J. McCourt, J. W. Curtis, E. A. Doucette, and S. S. Mehta

***Abstract*—The risk-aware path planning problem is considered, which aims to locate a target in a congested urban environment and facilitate aid in the decision making on target interdiction. The target is modeled as a ground vehicle moving randomly within a road network and following traffic rules. To locate the target, a heterogeneous sensor network composed of passive sensors (e.g., static traffic cameras and mobile human observers) and active sensors (e.g., a UAV) is tasked to cooperatively search for the target. A sample-based Bayesian filter is developed to fuse various sensor measurements to estimate the target state. To facilitate the decision making on target interdiction, a notion of risk is considered, which evaluates the incurred loss of target interdiction at certain locations based on incomplete information of target state and urban factors (e.g., the proximity to critical areas such as populated shopping malls, schools, military, or government buildings). As opposed to the static traffic cameras and the randomly walking human observers that passively provide target measurements, the UAV actively plans its path, based on mutual information, to maximize the informativeness of future measurements. In contrast to classical target tracking that only focuses on reducing the uncertainty of target state, the risk is encoded in the particle weights to guide the motion of UAV to improve target state estimation and, ultimately, reduce the risk of decision on target interdiction. Simulation results are provided to demonstrate the integrated sensing framework and the risk-aware path planning algorithm.**

I. Introduction

Networked agents that interact and cooperate as a team have the potential to perform various tasks, such as target classification and tracking, surveillance, reconnaissance, and scientific exploration [1]–[3]. Although homogeneous agents (i.e., the same type of agents) are widely used in such applications, system performance can be augmented by considering agents with heterogeneous capabilities, since certain type of agents may be better able to handle a set of tasks than others. For instance, in target search and tracking by a team composed of autonomous robots and human observers, autonomous robots equipped with advanced sensors (e.g., camera or Lidar) can provide more accurate estimates of the target position and velocity, while human observers generally do a better job in target classification and description (e.g., target type, size, or shape). However, ensuring proper coordination between heterogeneous agents and integrating information from various sources to improve system performance can be challenging.

In the context of estimation theory, target tracking can be viewed as estimation of target state given noisy measurements. One popular approach to nonlinear and non-Gaussian estimation is the particle filter framework, which represents the state uncertainty by a set of weighted samples (i.e., particles) and the sample weights are updated when new measurements are obtained [4]. The key advantage of particle filtering is that nonlinear system dynamics and nonlinear constraints can be accommodated in the particle filter framework, and the Bayesian optimal estimate can be approximated with sufficient number of particles [5]. Some earlier results using the particle filter in urban target tracking include Variable Structure Multiple Model Particle Filter using information from road maps in [6], joint tracking and identification of targets in [7], and discrete Gauss-Markov target dynamics based approach in [8]. Recent results reported in [9] and [10] develop particle filter based frameworks that integrate soft information sensors (e.g., verbal cues from human observers) with conventional information sensors (e.g., cameras) to improve estimation efficiency.

Information theoretic approaches have been used recently for active sensing in information gathering. Since mutual information can predict how much new sensor measurements will reduce the uncertainty of the target state, various mutual information based results are developed for efficient information seeking in target tracking. For instance, to minimize the expected uncertainty of the target state, a greedy optimization algorithm is developed in [11] that controls the mobile sensors to maximize the mutual information of the future sensor measurements and the target state. Entropy minimization based active sensing is addressed in [12], where a receding horizon control approach is used to minimize the posterior entropy. In [13], robots are controlled to build maps of radiation intensity based on mutual information methods. Sensor placement and informative trajectory planning are developed in [14]. In recent works of [15] and [16], information gradient based controllers are developed for a sensor network to infer the state of an environment such that the sensors move

Z. Kan and M. J. McCourt are with the Department of Mechanical and Aerospace Engineering, University of Florida, Gainesville, FL, USA. Email: {kanzhen0322, mccourt}@ufl.edu. C. Ton is with National Research Council, USA. Email: chau.t.ton@gmail.com. S. S. Mehta is with the Department of Industrial and Systems Engineering, University of Florida, Gainesville, FL, USA. Email: siddhart@ufl.edu. J. W. Curtis and E. A. Doucette are with the Munitions Directorate, Air Force Research Laboratory, Eglin AFB, FL, USA. Email: {jess.curtis, emily.doucette}@eglin.af.mil.

This research is supported in part by a grant from the AFRL Mathematical Modeling and Optimization Institute contracts #FA8651-08-D-0108/042–043 and the USDA NIFA AFRI National Robotics Initiative #2013-67021-21074. Any opinions, findings and conclusions or recommendations expressed in this material are those of the authors and do not necessarily reflect the views of the sponsoring agency.

978-1-4799-8697-2/15 $31.00 © 2015 IEEE
DOI 10.1109/SMC.2015.211

along the gradient of the mutual information to maximize the informativeness of future observations. However, most results developed in [11]–[16] are not immediately applicable for complex urban environments where obstacles and road maps impose constraints on the sensor motion.

In the present work, a heterogeneous sensor network composed of passive sensors (e.g., static traffic camera and mobile human observers) and a active sensor (e.g., a UAV) is tasked to locate a target in a congested urban environment and facilitate the decision making on target interdiction. The target is modeled as a ground vehicle moving randomly along the road network within an urban environment. It is assumed that certain intersections are equipped with traffic cameras that can detect the target from the traffic and provide periodic measurements. Human observers walking randomly along the road map can also report binary measurements on detection or non-detection of the target. The UAV actively plans its path based on where the next measurement should be taken to improve the estimation of target state and, ultimately, reduce the risk associated with target interdiction. To facilitate aid in the decision making on target interdiction in an urban environment, a notion of risk is considered, which evaluates the incurred loss from target interdiction based on incomplete information of target state and urban factors (e.g., the proximity to critical areas such as populated shopping malls, schools, military, or government buildings). When intercepting a target in an urban environment, the incurred risk (e.g., collateral damage) is highly location dependent. For instance, target interdiction near a populated shopping mall or school zone would incur far more loss than in a less populated zone. A hazard map associated with the urban environment is assumed to be known which indicates the potential risk of target interdiction at certain locations. A novel particle filter based Bayesian framework is developed to encode particle weights with the potential risk of decision on target interdiction and the uncertain measurements from traffic cameras, human observers, and UAV sensors, as well as Type I (i.e., false positive) and Type II error (i.e., false negative) associated with sensors. To facilitate active sensing, the classical mutual information based approach is modified to allow the UAV to plan its path to maximize the informativeness of future measurements, in terms of reducing the risk of decision on target interdiction. In addition, the a priori known urban attributes such as road speed limit, lanes, and traffic rules are included in the present work to define a more realistic path planning problem. Simulation results are then provided to demonstrate the integrated sensing framework and the risk-aware path planning algorithm.

II. Problem Formulation

A. Urban Environment and Target Model

Consider an urban environment $E_u \subset \mathbb{R}^2$ that consists of obstacles $E_o \subset \mathbb{R}^2$ (e.g., buildings) and the free space $E_f \subset \mathbb{R}^2$ (e.g., roads and intersections) with $E_o \cup E_f = E_u$. As shown in Fig. 1, the solid rectangular objects indicate the obstacles and the remaining area indicates the free space.

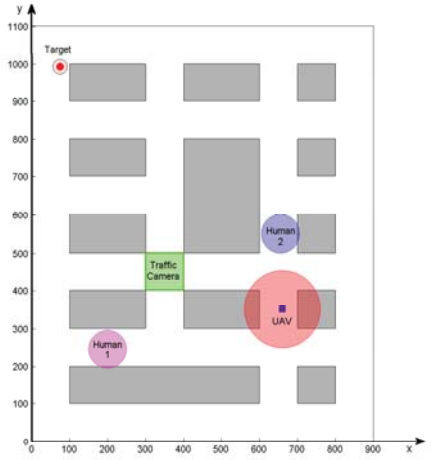

Figure 1. The urban target tracking scenario. The solid rectangles indicate obstacles (e.g., buildings) and the white space between obstacles indicate roads and intersections. The green rectangle indicates the field of view of the traffic camera at the selected intersection. The mobile target is represented by a red dot. The observation areas of two human observers are represented by a blue and a magenta disks, respectively. The sensing footprint of the UAV is represented by a red disk area.

It is assumed that full knowledge of the urban environment E_u (i.e., roads, buildings, intersections, and speed limits) is available. The target is modeled as a ground mobile vehicle with nonholonomic kinematic constraints as

$$\begin{aligned} p_k^x &= p_{k-1}^x + \Delta_t v_k \cos\theta_k \\ p_k^y &= p_{k-1}^y + \Delta_t v_k \sin\theta_k, \end{aligned} \tag{1}$$

where $\Delta_t \in \mathbb{R}^+$ is the discrete time step size, $x_T(k) \triangleq [p_k^x, p_k^y] \in \mathbb{R}^2$, $\theta_k \in \mathbb{R}$, and $v_k \in \mathbb{R}^+$ denote the target position, the target heading, and the target forward speed at time k, respectively. The target is assumed to move within the free space E_f (i.e., the target is not allowed to enter the obstacle space E_o or leave the map), traveling straight along the road and making turns randomly at intersections. The target is further restricted to remain on the right side of the road by following traffic flow and maintains a reasonable speed according to the associated road speed limit. To model the uncertainty in the target motion, its speed $\mathbf{v}_k$ is defined as $\mathbf{v}_k \triangleq V_r + \frac{u_k - 0.5}{5} V_r$, where $V_r \in \mathbb{R}^+$ denotes the associated road speed limit and $u_k \in [0,\, 1]$ is a random number drawn from the uniform distribution $\mathcal{U}(0, 1)$. The target position at time k is denoted by a random variable $\mathbf{x}_T(k) \in \mathbb{R}^2$ and $\mathcal{X} \subset E_f$ represent the state space of $\mathbf{x}_T$. The particle filter is used in the present work to represent the probability distribution of the target position. The key idea of the particle filter is to use a set of independent random samples, also called *particles*, to represent the posterior distribution of a system state (cf. [17] and [4]). As a new sequence of sensor measurements arrives, the particles are re-weighted to update the state estimate.

B. Sensors

A heterogeneous sensor network that consists of passive sensors and active sensors provides measurements of the moving target in an obstacle-rich urban environment. As shown in Fig. 1, the field-of-view (FOV) of the traffic camera covers the entire intersection. The disks in Fig. 1 represent the observation areas of two human observers and the sensing footprint of the UAV.

Consider $n_c \in \mathbb{Z}^+$ cameras located at road intersections and let $\psi_c^i \in \mathbb{R}^2$, $i \in \{1, \ldots, n_c\}$, be the FOV of the ith traffic camera. The traffic cameras are assumed to provide measurements to report detection or non-detection of the target. Particularly, if $\mathbf{x}_T(k) \in \psi_c^i$, the measurement $\mathbf{m}_{c,k}^i$ received from the camera i at time k is modeled as a Bernoulli random variable

$$\mathbf{m}_{c,k}^i = \begin{cases} 1 & \text{with probability } p_c^i \\ 0 & \text{with probability } 1 - p_c^i, \end{cases} \tag{2}$$

where $\mathbf{m}_{c,k}^i = 1$ and $\mathbf{m}_{c,k}^i = 0$ indicates a detection and non-detection reported by camera i, respectively. The $p_c^i \in (0,\, 1)$ in (2) indicates the probability of reporting detection if the target is within the FOV of camera i. Similarly, if $\mathbf{x}_T(k) \notin \psi_c^i$,

$$\mathbf{m}_{c,k}^i = \begin{cases} 1 & \text{with probability } 1 - q_c^i \\ 0 & \text{with probability } q_c^i, \end{cases} \tag{3}$$

where $q_c^i \in (0,\, 1)$ in (3) indicates the probability of reporting non-detection if the target is not within the FOV of camera i. The probability $1 - p_c^i$ in (2) and the probability $1 - q_c^i$ in (3) are also known as Type II error (i.e., false negative) and Type I error (i.e., false positive), respectively.

Human observers are involved by acting as mobile sensors walking randomly along the road map. Consider $n_h \in \mathbb{Z}^+$ human observers and assume the observation area of each human $i \in \{1, \ldots, n_k\}$ is a disk area $\psi_h^i \in \mathbb{R}^2$ with radius $r_h^i \in \mathbb{R}^+$, as shown in Fig. 1. Although humans can provide rich description of the target by naturally encoding their observations (e.g., target size, color, type, etc.) as in our earlier work of [10], a simplified sensing model for humans is applied in the current work, where humans only report detection or non-detection of the target as they randomly walk in the the urban environment E_u. Ongoing work is to fuse human sensing information via touch interface to improve the target estimate. Similar to traffic cameras, a target classification error is also associated with the human observers, due to imperfect visual and cognitive abilities. The measurement $\mathbf{m}_{h,k}^i$ from human i at time k, similar to (2) and (3), is modeled as a Bernoulli random variable, where $\mathbf{m}_{h,k}^i = 1$ with probability $p_h^i \in (0,\, 1)$ and $\mathbf{m}_{h,k}^i = 0$ with probability $1 - p_h^i$ given that $\mathbf{x}_T(k) \in \psi_h^i$. If $\mathbf{x}_T(k) \notin \psi_h^i$, $\mathbf{m}_{h,k}^i = 0$ with probability $q_h^i \in (0,\, 1)$ and $\mathbf{m}_{h,k}^i = 1$ with probability $1 - q_h^i$.

A fixed wing UAV with constant velocity and altitude is utilized throughout the work. Similar to traffic cameras and human observers, the UAV sensor (e.g., a down-looking monocular camera) also reports detection or non-detection of the target, with a sensor footprint projected on E_u modeled as a disk area $\psi_{UAV} \in \mathbb{R}^2$ with radius $r_{UAV} \in \mathbb{R}^+$. The measurements from the UAV sensor $\mathbf{m}_{UAV,k}$ at time k follow a similar distribution as in (2) and (3), where $\mathbf{m}_{UAV,k} = 1$ with probability $p_{UAV} \in (0,\, 1)$ and $\mathbf{m}_{UAV,k} = 0$ with probability $1 - p_{UAV}$ given that $\mathbf{x}_T(k) \in \psi_{UAV}$. If $\mathbf{x}_T(k) \notin \psi_{UAV}$, $\mathbf{m}_{UAV,k} = 0$ with probability $q_{UAV} \in (0,\, 1)$ and $\mathbf{m}_{UAV,k} = 1$ with probability $1 - q_{UAV}$. While static traffic cameras and randomly walking human observers passively receive target measurements, the UAV actively plans its path on where the next measurement should be taken such that the target estimate can be improved, using the particle filter based target probability distribution.

C. Target Interdiction Risk

Let $L(l,\, x_T(k)) : E_u \times \mathcal{X} \to \mathbb{R}$ denote a known measure of loss at time k when intercepting the target at a certain location $l \in E_f$ given a certain target position $x_T(k) \in \mathcal{X}$. It is assumed that environment factors such as critical buildings or populated areas are encoded in the function $L(l,\, x_T(k))$. For instance, larger loss will be incurred if the target is intercepted near populated areas (e.g., shopping mall or school zone) or close to critical buildings (e.g., hospitals, military, or government buildings). Given the belief of target position probability distribution $\Pr(\mathbf{x}_k)$ at time k, the expected loss of target interdiction at location l is defined as $R_k(l) = \int_{x_k \in \mathcal{X}} L(l,\, x_k) \Pr(x_k)\, dx_k$, which can be approximated as

$$R_k(l) = \sum_{i=1}^{N} L\left(l,\, \mathbf{x}_k^{(i)}\right) \Pr\left(\mathbf{x}_k^{(i)}\right), \tag{4}$$

since the target state is estimated by weighted particles. In (4), the expected loss will be referred as *risk*, since it indicates how much loss we will experience with the expectation of target interdiction at location l given the belief of target states at time k. In contrast to most existing works that only focus on moving sensors to reduce uncertainty of the target estimation, the main objective in this work is to develop a path planning rule that actively guides the motion of the UAV to reduce the risk of decision on target interdiction.

III. Sample-based Bayesian Filter

Urban path planning relies on the information collected by traffic cameras, human observers, and UAV sensors, which necessitates the use of a sample-based Bayesian filter to fuse measurements from various sources. In the present work, a set of N particles are updated according to the target dynamics in (1) and the particle weights $\left\{w_k^{(i)}\right\}$ are updated according to the sensor measurements. Since the sensors are modeled in Section II, for simplicity in presentation, a common notation $\mathbf{z}_k$ will be used in the subsequent development to indicate the measurements from corresponding sensors. In particular, given the measurement $\mathbf{z}_k = 1$ at time k,

which indicates a detection of the target from either the traffic camera, UAV sensor, or human observer, the probability that the target exists in the corresponding sensor footprint (i.e., $\mathbf{x}_T(k) \in \psi$) is

$$\begin{aligned} \Pr(\mathbf{x}_T(k) \in \psi | \mathbf{z}_k = 1) &= \xi \\ \Pr(\mathbf{x}_T(k) \notin \psi | \mathbf{z}_k = 1) &= 1 - \xi, \end{aligned} \tag{5}$$

where $\psi \in \{\psi_c, \psi_h, \psi_{UAV}\}$ is a generalized sensor footprint and $\xi \in (0, 1)$ is the probability that the target is present in the corresponding sensor footprint given the measurement of detection. Since the measurement of detection does not ensure the target presence in ψ from (5), it is desirable to maintain non-zero mass of particles outside ψ to account for Type I error. Using the error probabilities, the particle weight can be updated using Bayes rule as

$$w_k^{(i)} = \begin{cases} \frac{w_{k-1}^{(i)} \Pr\left(\mathbf{z}_k=1|\mathbf{x}_k^{(i)}\right)}{\sum_{j=1}^{N_1} w_{k-1}^{(j)} \Pr\left(\mathbf{z}_k=1|\mathbf{x}_k^{(j)}\right) + \sum_{N_1+1}^{N} w_{k-1}^{(j)}(1-\xi)}, & \mathbf{x}_k^{(i)} \in \psi \\ \frac{w_{k-1}^{(i)}(1-\xi)}{\sum_{j=1}^{N_1} w_{k-1}^{(j)} \Pr\left(\mathbf{z}_k=1|\mathbf{x}_k^{(j)}\right) + \sum_{N_1+1}^{N} w_{k-1}^{(j)}(1-\xi)}, & \mathbf{x}_k^{(i)} \notin \psi \end{cases} \tag{6}$$

where N_1 is the number of particles such that $\mathbf{x}_k^{(i)} \in \psi$, $\forall i \in \{1, \ldots, N_1\}$, and $\Pr\left(\mathbf{z}_k = 1 | \mathbf{x}_k^{(i)}\right)$ is the likelihood of reporting detection when $\mathbf{x}_k^{(i)} \in \psi$. The update law in (6) indicates that the weights of particles outside ψ will decrease with successive positive sensor measurements resulting in improved confidence of sensors against Type I error.

Analogously, due to Type II error, the probability that the target exists in the corresponding sensor footprint (i.e., $\mathbf{x}_T(k) \in \psi$) given the measurement of non-detection of target (i.e., $\mathbf{z}_k = 0$) at time k is

$$\begin{aligned} \Pr(\mathbf{x}_k \in \psi | \mathbf{z}_k = 0) &= \mu \\ \Pr(\mathbf{x}_k \notin \psi | \mathbf{z}_k = 0) &= 1 - \mu, \end{aligned} \tag{7}$$

where $\mu \in (0, 1)$ is the probability that the target is present given the measurement of non-detection. Since the measurement of non-detection does not guarantee the absence of the target in the sensor footprint, the particle update law is developed for the case of missed detection as

$$w_k^{(i)} = \begin{cases} \frac{\mu w_{k-1}^{(i)}}{\sum_{j=1}^{N_2} \mu w_{k-1}^{(j)} + \sum_{N_2+1}^{N} w_{k-1}^{(j)}}, & \mathbf{x}_k^{(i)} \in \psi \\ \frac{w_{k-1}^{(i)}}{\sum_{j=1}^{N_2} \mu w_{k-1}^{(j)} + \sum_{N_2+1}^{N} w_{k-1}^{(j)}}, & \mathbf{x}_k^{(i)} \notin \psi \end{cases} \tag{8}$$

where N_2 is the number of particles within ψ. The update law in (8) indicates that the weights of particles inside ψ will decrease with successive sensor measurements to safeguard against Type II error.

Note that the update laws in (6) and (8) aim to reduce the uncertainty of the target state estimate using sensor measurements, without considering the risk associated with target interdiction. Based on (6) and (8), the particle weights need to be further updated to encode the risk of target interdiction from (4). In particular, the urban environment E_u is divided into $c_m \times c_n$ block of cells in the present work, where each cell is denoted by $\mathcal{C}_{ij} \in E_u$ with $i \in \{1, \ldots, c_m\}$ and $j \in \{1, \ldots, c_n\}$. It is assumed that the urban environment is associated with a hazard map $H \in \mathbb{R}^{c_m \times c_n}$, where each entry $H_{ij} \in \mathbb{R}$ indicates a potential loss associated with target interdiction at $\mathcal{C}_{ij}$. For instance, higher loss value H_{ij} is assigned to the cell $\mathcal{C}_{ij}$ that contains critical areas such as schools, military or government buildings. Given the estimated target distribution at time k, the risk value $R_k(\mathcal{C}_{ij})$ in (4) indicates the incurred loss if the decision is made to intercept the target at cell $\mathcal{C}_{ij}$. An example $R_k(\mathcal{C}_{ij})$ used in the current work is in the form of

$$R_k(\mathcal{C}_{ij}) \triangleq \alpha \sum_{m \notin I_k^{ij}} w_k^{(m)} + \beta H_{ij}, \tag{9}$$

where I_k^{ij} denotes the set of particle indices such that $\mathbf{x}_k^{(m)} \in \mathcal{C}_{ij}$ for $\forall m \in I_k^{ij}$ and $\alpha, \beta \in \mathbb{R}^+$ are weighting factors to adjust the relative importance of target uncertainty represented by particles and the potential loss represented by the hazard map. Based on (9), new particle weights $\left\{\mathbf{x}_k^{(i)}, \zeta_k^{(i)}\right\}$ are created with

$$\zeta_k^{(i)} = \frac{w_k^{(i)}}{R_k(\mathcal{C}_{ij})}, \quad \forall i \in I_k^{ij}, \tag{10}$$

where the particles weights are rescaled based on the risk values computed from (9). The update law in (9) indicates that the particles within high-risk areas will decrease their weights, since there is less reward for target interdiction in high-risk areas. After performing (10), all weights of particles are then normalized to satisfy $\sum_{i=1}^{N} \zeta_k^{(i)} = 1$. Resampling of particle weights is applied when necessary to avoid the degeneracy phenomenon [4].

IV. Risk-aware Path Planning

In Information Theory [18], the entropy of a probability distribution $\Pr(\mathbf{x}_k)$ is a measure of its uncertainty, which is defined as $H(\mathbf{x}_k) \triangleq -\int_{x_k \in \mathcal{X}} \Pr(x_k) \log \Pr(x_k) dx_k$, where $\mathcal{X}$ is the state space of $\mathbf{x}_k$. The mutual information between the state $\mathbf{x}_k$ and the measurement $\mathbf{z}_k$ is then defined as

$$I_k \triangleq \int_{z_k \in \mathcal{Z}} \int_{x_k \in \mathcal{X}} \Pr(x_k, z_k) \log \frac{\Pr(x_k, z_k)}{\Pr(x_k) \Pr(z_k)} dx_k dz_k \tag{11}$$

where $\mathcal{Z}$ is the state space of $\mathbf{z}_k$. In (11), the mutual information is a metric of the expected divergence (Kullback-Liebler) between $\mathbf{x}_k$ and $\mathbf{z}_k$, which indicates how much information one random variable can provide on the other. Since the state $\mathbf{x}_k$ in the current work is represented by a set of particles that encodes target state uncertainty and the risk associated with target interdiction, inspired by the mutual information, it is desirable to move the UAV in a way to maximize the mutual information such that its future

measurements can provide as much information on $\mathbf{x}_k$ as possible.

In particular, the UAV plans its path by selecting a specific road to proceed from a set of permissible roads when reaching an intersection. Since the UAV is constrained to move forward within the road network and is not allowed to stay on the map or fly backward, the permissible roads at each intersection contains up to three candidates, which restricts the UAV to either go straight, turn left, or turn right, depending on the road network. Based on the mutual information in (11), the path is determined by selecting a specific road that can maximize the predicted mutual information. The predicted mutual information is calculated for each candidate permissible road by propagating the particles forward in time under the assumption that no new measurements are available from all sensors. The path planning decision is then made based on a greedy approach by selecting a candidate road that provides the most predicted mutual information.

It is assumed that the UAV has complete knowledge of the urban environment such as all obstacles, roads, and intersections, which enables the UAV to know immediately the set of permissible roads and the distance to the permissible roads when reaching an intersection. Consider that all intersections are labeled and let the ith permissible road be r_i, $i \in I_j^R$, where I_j^R represents the set of indices of permissible roads at the jth intersection. Since the UAV moves with constant velocity, the travel time t_i from its current position to the road r_i is available. The predicted mutual information obtained by assuming the UAV at the road r_i is calculated by propagating the particles for a amount of time t_i from the current time k to $k' = k + t_i$. Using the predicted particles $\left\{\mathbf{x}_{k'}^{(i)}, \zeta_{k'}^{(i)}\right\}$, the predicted mutual information for road r_i can be approximated from (11) as

$$I_{k'}(r_i) = \sum_{z_k \in \mathcal{Z}} \sum_{i=1}^{N} \Pr\left(\mathbf{z}_{k'} = z_{k'} | \, \mathbf{x}_{k'} = x_{k'}^{(i)}\right) \zeta_{k'}^{(j)} \times \log\left(\frac{\Pr\left(\mathbf{z}_{k'} = z_{k'} | \, \mathbf{x}_{k'} = x_{k'}^{(i)}\right)}{\sum_{j=1}^{N} \zeta_{k'}^{(j)} \Pr\left(\mathbf{z}_{k'} = z_{k'} | \, \mathbf{x}_{k'} = x_{k'}^{(j)}\right)}\right), \tag{12}$$

where the likelihood $\Pr\left(\mathbf{z}_{k'} = z_{k'} | \, \mathbf{x}_{k'} = x_{k'}^{(i)}\right)$ is assumed known for calibrated UAV sensors. Based on (12), the subsequent road for the UAV at the jth intersection is determined by

$$r = \arg\max_{r_i} I_{k'}(r_i), \quad \forall i \in I_j^R, \tag{13}$$

which indicates that the UAV selects a path with maximum predicted mutual information. Since $I_k(r_i)$ in (12) is computed based on an assessment of the predicted mutual information on immediately subsequent roads, the decision policy (i.e., one-step decision) in (13) may suffer from its myopic construction. Ongoing work considers a better decision making policy using Partially Observed Markov Decision Process (POMDP) based approaches for multi-step decision in the UAV path planning (cf. [19]).

V. Simulation Results

Simulation results are provided to demonstrate the performance of the developed path planning framework. Based on the urban environment described in Section II, the initial positions of the target, human observers, and the UAV are randomly selected from the free space E_f, and their initial headings are determined based on the traffic flow of the selected initial positions. The sensing radius of the human observers and the UAV are set as 45 m and 100 m, respectively. To represent Type I and Type II error associated with the sensors, the probability of false positive and false negative are set as 0.05 and 0.2. The road speed limit is set as 30 miles/hour and the target moves according to (1) within the road map following traffic rules. Human observers and the UAV move with a fixed speed of 5 miles/hour and 40 miles/hour, respectively. The environment is divided into 11×9 grid of square cells, where each cell has a size of $100 \text{ m} \times 100 \text{ m}$.

To represent the initial estimate of the target position, a set of 1000 particles with equal weights are uniformly and randomly deployed on the roads in E_u. The critical area is indicated in Fig. 2, where the associated hazard map is represented by the colored area around the critical area. The hazard level is encoded according to the color bar, where red indicates a potential high loss associated with target interdiction. Based on the hazard map and the initially deployed particles, the risk based initial belief of the target distribution computed from (9) is represented in Fig. 3, where the value indicates the accumulated particle weights that encode the target uncertainty and the risk of target interdiction at corresponding locations. As shown in Fig. 3, the area around the critical area is associated with low values, which indicates visiting that area may not provide much information to reduce the risk associated with the decision on target interdiction. Based on the developed path planning algorithm, the UAV plans its path to reduce the risk of target interdiction, where Fig. 4 indicates an example trial where the estimated entropy and the minimal risk decrease on average during the simulation. To show the average performance, 50 Monte Carlo trials were conducted with the same initial positions and headings for the target, human observers, and the UAV. For each trial, the particles are randomly deployed initially and the target moves along a random and unknown trajectory. Each trial duration is restricted to 100 seconds. Simulation results show that the average reduction of estimate entropy is 54%. To show that the performance of the developed path planning algorithm, the minimal risk value for each trial is recorded and the average reduction of minimal risk value is 43%, which indicates that the UAV moves in a way to improve the performance of urban target estimate and interdiction.

VI. Conclusion

This paper examines the urban path planning problem that consists of passive sensors (e.g., static traffic camera and mobile human observers) and active sensors (e.g., a

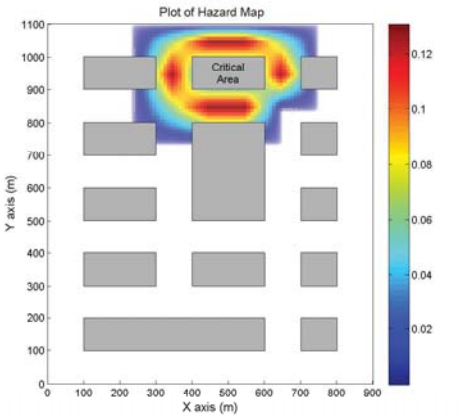

Figure 2. The plot of hazard map around the critical area.

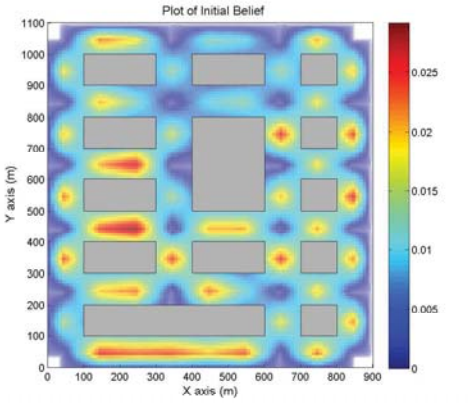

Figure 3. The plot of the risk based belief on the target distribution.

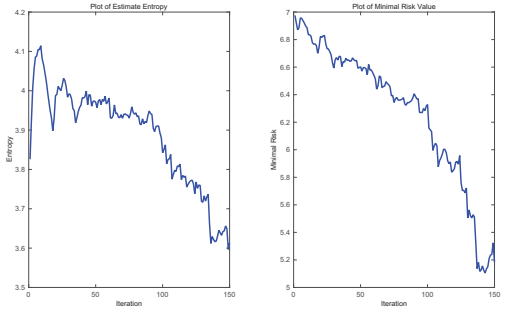

Figure 4. The left plot shows the decrease of estimate entropy and the right plot shows the decrease of the minimal risk value during evolution.

UAV). A sample-based Bayesian filter is developed to fuse various sensor measurements to improve the target estimate. A simplified human model that only reports detection or non-detection of the target is used in the present work. Future work will consider an advanced human model that can provide rich information about the target by voice, text, or user-interface to improve target classification and tracking. Future work will also consider multi-step decision policies for the UAV path planning using Partially Observed Markov Decision Process (POMDP) based approaches.

REFERENCES

[1] S. Ponda, N. Ahmed, B. Luders, E. Sample, T. Hoossainy, D. Shah, M. Campbell, and J. P. How, "Decentralized information-rich planning and hybrid sensor fusion for uncertainty reduction in human-robot missions," in *AIAA Guid., Naviga., and Control Conf.*, Portand, OR, Aug 2011, pp. 1–22.

[2] Z. Kan, E. L. Pasiliao, J. W. Curtis, and W. E. Dixon, "Particle filter based average consensus target tracking with preservation of network connectivity," in *Proc. IEEE Mil. Commun. Conf.*, 2012, pp. 760–765.

[3] D. E. Soltero, M. Schwager, and D. Rus, "Decentralized path planning for coverage tasks using gradient descent adaptive control," *Int. J. Robot. Res.*, pp. 1–25, 2013.

[4] N. Gordon, D. Salmond, and A. Smith, "Novel approach to nonlinear/non-gaussian bayesian state estimation," in *IEE Proc. Radar and Signal Process.*, vol. 140, no. 2. IET, 1993, pp. 107–113.

[5] D. Simon, "Kalman filtering with state constraints: a survey of linear and nonlinear algorithms," *IET Control Theory & Appl.*, vol. 4, no. 8, pp. 1303–1318, 2010.

[6] M. S. Arulampalam, N. Gordon, M. Orton, and B. Ristic, "A variable structure multiple model particle filter for GMTI tracking," in *Int. Conf. Inf. Fusion*, vol. 2. IEEE, 2002, pp. 927–934.

[7] C. S. Agate and K. J. Sullivan, "Road-constrained target tracking and identification using a particle filter," in *Proc. of SPIE Conf. Signal Data Process. Small Target*, vol. 5204, 2003, pp. 532–543.

[8] M. Ulmke and W. Koch, "Road-map assisted ground moving target tracking," *IEEE Trans. Aerosp. Electron. Syst.*, vol. 42, no. 4, pp. 1264–1274, 2006.

[9] S. S. Mehta, P. E. K. Berg-Yuen, E. L. Pasiliao, and R. A. Murphey, "A control architecture for human-machine interaction in the presence of unreliable automation and operator cognitive limitations," in *AIAA Guidance, Navigation and Control (GNC) Conference*, Minneapolis, MN, 2012, in review.

[10] S. Mehta, M. McCourt, E. Doucette, and J. Curtis, "A touch interface for soft data modeling in Bayesian estimation," in *IEEE Int. Conf. on Systems, Man, and Cybernetics*. IEEE, 2014, pp. 3732–3737.

[11] G. M. Hoffmann and C. J. Tomlin, "Mobile sensor network control using mutual information methods and particle filters," *IEEE Trans. Autom. Control*, vol. 55, no. 1, pp. 32–47, 2010.

[12] A. Ryan and J. K. Hedrick, "Particle filter based information-theoretic active sensing," *Robot. Auton. Syst.*, vol. 58, no. 5, pp. 574–584, 2010.

[13] R. A. Cortez, H. G. Tanner, R. Lumia, and C. T. Abdallah, "Information surfing for radiation map building," *Int. J. Robot. Autom.*, vol. 26, no. 1, pp. 4–12, 2011.

[14] H.-L. Choi and J. P. How, "Efficient targeting of sensor networks for large-scale systems," *IEEE Trans. Control Syst. Techno.*, vol. 19, no. 6, pp. 1569–1577, 2011.

[15] M. Schwager, P. Dames, D. Rus, and V. Kumar, "A multi-robot control policy for information gathering in the presence of unknown hazards," in *Int. Symp. Robot. Res.*, 2011.

[16] B. J. Julian, M. Angermann, M. Schwager, and D. Rus, "Distributed robotic sensor networks: An information-theoretic approach," *Int. J. Robot. Res.*, vol. 31, no. 10, pp. 1134–1154, 2012.

[17] M. Arulampalam, S. Maskell, N. Gordon, and T. Clapp, "A tutorial on particle filters for online nonlinear/non-gaussian bayesian tracking," *IEEE Trans. Signal Process.*, vol. 50, no. 2, pp. 174–188, 2002.

[18] T. M. Cover and J. A. Thomas, *Elements of information theory*. John Wiley and Sons, 2012.

[19] E. K. Chong and S. H. Zak, *An introduction to optimization*. John Wiley & Sons, 2013, vol. 76.